

## On the Influence of Radiation on Local Extinction in a Turbulent Non-Premixed Methane Flame

Guenther C. Krieger Filho

University of São Paulo

e-mail: guenther@usp.br

**Abstract.** *The structure of a nonpremixed turbulent methane flame is investigated in this work. Special emphasis is given to the influence of radiation on the local extinction phenomena. The numerical simulation is performed with PDF method enhanced with the algorithm "in situ adaptive tabulation" (ISAT). The ISAT method avoids both, the memory consuming look-up table, and the time consuming integration of differential equations of the chemical reactions. The chemistry is described by a reduced mechanism with 10 global reactions and 14 species. Radiation heat losses are accounted for by retaining the radiation source term in the energy equation. The flame is assumed to be optically thin. The coupling between thermo-chemistry and turbulence models is done using a PDF-Method and a conventional CFD code. The flame structure is investigated by means of average value and conditioned average values of temperature and CO concentration. The numerical results are compared with experimental data. It is verified that the profiles of averaged quantities such as mixture fraction, temperature and major species concentrations are in acceptable agreement with the experimental data. Beside the mean value of temperature and major concentrations, conditioned mean values are also presented. It can be seen that partial extinction is very pronounced in the near nozzle region, where the Damköhler Number is low. The influence of radiation can be seen on the temperature profiles CO and CO<sub>2</sub> profiles. The effects of radiation are, however only marginal. Both models, with and without radiation effects, show a similar description of the whole combustion process in comparison with the experimental data.*

**keywords:** *Combustion, Extinction, Non-premixed, Radiation, Methane.*

### 1. Introduction

Turbulent non-premixed flames are very important for industrial applications. In particular, methane flames are specially important, since methane is known to be the major component of natural gas. Moreover, a better understanding of the process of pollutant formation in such flames is fundamental for designing burners and furnaces with low emissions. However, to achieve this goal one has to use detailed chemistry and also radiation. On the other hand, CFD codes have become lately an useful tool for combustion modeling. However, the efficiency and reliability of these codes depend on how accurate their combustion models are. The most challenging aspect in dealing with turbulent reactive flows is how to treat chemistry and radiation. A combustion model including detailed chemistry involves solving a large number of nonlinear differential equations that are notoriously stiff, owing to the fact that reactions cover a wide range of time scales (Kuo, 1986). Furthermore, the radiation heat transfer in the flame brings more complexity to the model. The radiation source term is, like the chemical source term, also non-linear and its interaction with the turbulent fluctuations of temperature and concentrations has to be taken into account. Extensive experimental work was carried out by (Turns and Myhr, 1975) to understand the interrelationships among NO<sub>x</sub>, flow conditions and flame radiation. They have studied hydrocarbon turbulent nonpremixed flames. The effects of flow parameters and fuel type on radiant losses are shown to be important in determining the NO<sub>x</sub> emissions from simple jet hydrocarbon flames. In the present study, detailed chemistry and radiation heat transfer are used to model a turbulent non-premixed methane flame. The ISAT algorithm (Pope, 1997), which is described below, was implemented with the PDF method and enables the use of a detailed chemistry mechanism with radiation source term. Local flame extinction plays a very important role as far as both pollutant formation and combustion stability are concerned.

### 2. Objectives

The main goal of the present study is to evaluate the influence of radiation on the local extinction in a turbulent diffusion methane flame. In order to do this, the ISAT algorithm is implemented together with a detailed chemistry and radiation model. The present work completes the previous one (Krieger, 2002), where the investigations were carried out without the radiation model. Commonly used turbulent combustion models

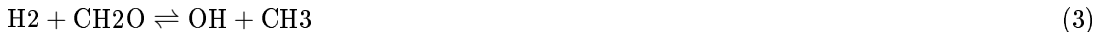
(Janicka and Kollmann, 1979; Magnussen and Hjertager, 1976) are not able to give information about local extinction in the flame, therefore PDF/ISAT Method was used here.

### 3. Flame

The combustion system investigated is a vertical free jet turbulent diffusion flame. The fuel is a mixture of three parts air and one part CH<sub>4</sub>. This mixture significantly reduces the problem of fluorescence interference from soot precursors, allowing improved accuracy in the scalar measurements. Partial premixing with air also reduces the flame length and produces a more robust flame than pure CH<sub>4</sub>. The mixing rates are high enough that this flame burns as diffusion flame, with a single reaction zone near the stoichiometric mixture fraction and no evidence of premixed reaction in the fuel-rich CH<sub>4</sub>/air mixtures. The burner nozzle has a diameter of 7.2 mm. The Reynolds number of the main jet is 22400. The flame is stabilized with pilots. The pilot is a lean premixture of C<sub>2</sub>H<sub>2</sub>, H<sub>2</sub>, air, CO<sub>2</sub>, and N<sub>2</sub> with the same nominal enthalpy and equilibrium composition as methane/air at this equivalence ratio. The energy release of the pilot is approximately 6% of the main jet. This flame is proposed by International Workshop on Measurement and Computation of Non-premixed Flames (TNF, 1999b) as a well documented test-case for combustion modeling.

### 4. Thermochemical Model

The methane combustion model adopted in the present work was proposed by (Chen, 1997) and recommended by the International Workshop on Measurement and Computation of Non-premixed Flames (TNF, 1999b). Starting from a skeletal mechanism containing 172 elementary reactions involving C1 and C2 chains, a reduced mechanism containing 10 steps or pseudo-global reactions is obtained. The reduction strategy can be seen in (Chen, 1997). The basic idea of the strategy is to identify minor species that can be assumed as being in steady state. For these minor species, the model uses algebraic relations rather than ordinary differential equations (ODE). For the remaining species a set of ODEs is formulated as function of formation/destruction kinetic rates. The reduced mechanism used in this work contains 14 species: O<sub>2</sub>, H, OH, H<sub>2</sub>, H<sub>2</sub>O, CO, CO<sub>2</sub>, CH<sub>3</sub>, CH<sub>2</sub>O, C<sub>2</sub>H<sub>2</sub>, C<sub>2</sub>H<sub>4</sub>, C<sub>2</sub>H<sub>6</sub>, CH<sub>4</sub> and N<sub>2</sub>. However, Nitrogen is considered as inert in the combustion process. No attention is given here to NO formation. This should be done in a future work, after evaluating the capability of the PDF/ISAT mechanisms to predict minor species like CO. The mechanism is constituted by the following pseudo-global reactions:



The net formation/destruction rate for each of the species above was computed with the routine CKWYP10.f, which was developed by (Chen, 1997) and is available on the Web at TNF, 1999b. The thermochemical model models the mixture as an ideal gas at atmospheric pressure.

### 5. Radiation Model

The main goal of the present work is to evaluate the influence of radiative losses on the turbulent flame structure, particularly on the local extinction. The radiation model is based upon the assumption of optically thin radiative transfer between a given fluid element in the flame and the cold surroundings. The radiation

source term in the energy transport equation is given by

$$\dot{q} = 4\sigma(T^4 - T_b^4) \sum_i p_i a_{p,i}, \quad (12)$$

where  $\sigma = 5.669E^{-8} W/m^2 K^4$ ,  $T$  is the local flame temperature,  $T_b$  is the background temperature,  $p_i$  is the partial pressure of species  $i$  in atmospheres, and  $a_{p,i}$  is the Planck mean absorption coefficient for species  $i$ . In the present work only the  $H_2O$  and  $CO_2$  molecules were taken into account as radiative species. The Planck mean absorption coefficient for these species were taken from Barlow, 2001.

## 6. Turbulent Combustion Model

The thermochemical being used model was described in the previous section. In this mechanism, there appears 14 chemical species, which would require the solution of fourteen turbulent transport equations. The solution of these coupled transport equations is a formidable task, if done by usual approaches. In the moment closure method the difficulty lies in formulating appropriate average chemical source terms and in modeling scalar-velocities correlations. This makes the moment closure method not feasible for complex chemistry models. In PDF Methods one has the problem of storage and management of look up tables (Hinz, 2000) in which compositions and temperature are pre-processed. In the present work, the PDF method was implemented with the In Situ Algorithm Tabulation (ISAT) proposed by Pope, 1997. With this algorithm, it was possible to model the turbulent methane flame with the detailed chemistry model already described. The PDF/ISAT method is described shortly in the following. In turbulent flows the variables assume a random behavior. Hence, simulation methods need to use a statistical approach to the problem. In such an approach, only statistical moments of certain variables are evaluated, such as mean value and variance. Then, a question remains as to how one goes from statistical moments of a variable to its instantaneous values, which are necessary in the thermochemical model. The answer is to compute a joint probability density function (PDF) of the scalar quantities (species and enthalpy) in the thermochemical model. This PDF couples the thermochemical model and the turbulent reactive flow model. If the PDF is known, average values can be evaluated as follows

$$\langle \phi \rangle = \int_{-\infty}^{+\infty} \phi(\psi) \mathbf{P}_\phi \mathbf{d}\psi, \quad (13)$$

where  $\psi$  is the sample space,  $P_\phi$  is the PDF,  $\phi(\psi)$  is the instantaneous value of a function  $\phi$  dependent on  $\psi$  and  $\langle \phi \rangle$  is its average value. The integration of the PDF over the sample space of scalars and velocities,  $\int \int P_{u,\phi} d\mathbf{v} d\psi$ , gives the probability that the velocity vector  $u$  at any time  $t$  and any position  $x$  is in the interval between  $\mathbf{v}$  and  $\mathbf{v} + d\mathbf{v}$  and simultaneously the vector of the scalars quantities  $\phi$  in the interval between  $\psi$  and  $\psi + d\psi$ . The PDF can be evaluated using two different methods. The first one consists in assuming a form for it beforehand. This approach is called presumed PDF (Kuo, 1986). The second one is based on the formulation, modeling and solution of the PDF transport equation. This approach was proposed by Pope, 1985 and is used in the present work. In the PDF-Method, the transport equation for the PDF is formulated, starting from the instantaneous conservation equation for mass, momentum, energy and chemical species. After some manipulation of the basic equations and applying statistical operators, one obtains the transport equation for the PDF  $P_{u\psi}$

$$\begin{aligned} \frac{\partial}{\partial t} \rho P_{u\phi}(\mathbf{v}, \psi; \mathbf{x}, \mathbf{t}) &+ \frac{\partial}{\partial x_i} \rho U_i P_{u\phi}(\mathbf{v}, \psi; \mathbf{x}, \mathbf{t}) + \frac{\partial}{\partial v_j} \left[ -P_{u\phi}(\mathbf{v}, \psi; \mathbf{x}, \mathbf{t}) \frac{\partial \bar{p}}{\partial x_j} \right] + \\ &\sum_{\alpha=1}^{N_\alpha} \frac{\partial}{\partial \psi_\alpha} [P_{u\phi}(\mathbf{v}, \psi; \mathbf{x}, \mathbf{t}) \rho \mathbf{S}_\alpha] = \sum_{\alpha=1}^{N_\alpha} \frac{\partial}{\partial \psi_\alpha} \left[ P_{u\phi}(\mathbf{v}, \psi; \mathbf{x}, \mathbf{t}) \left\langle \frac{\partial \mathbf{J}_{1\alpha}}{\partial x_i} \right\rangle_{\mathbf{v}, \psi} \right] + \\ &\frac{\partial}{\partial v_j} \left[ P_{u\phi}(\mathbf{v}, \psi; \mathbf{x}, \mathbf{t}) \left\langle -\frac{\partial \tau_{ij}}{\partial x_i} + \frac{\partial \mathbf{p}'}{\partial x_j} \right\rangle \right] \end{aligned} \quad (14)$$

In Eq. 14 above, the first term on the LHS represents the temporal variation of  $P_{u\psi}$  within the control volume, the second term gives the convective transport of  $P_{u\psi}$  in the physical space. The third term describes the transport of the PDF in the velocities space due to the gradient of mean pressure and the fourth term the transport in the scalar quantities space due to the chemical and radiation source terms. It is important to emphasize that, for a given value of  $P_{u\psi}$  all the terms in the LHS of Eq. 14 are either known or can be directly evaluated. On the RHS of Eq. 14 there are two terms describing transport on the scalar quantities and velocities spaces. These terms arise from molecular transport and pressure fluctuations in the instantaneous conservation equations. The two terms contain conditional averages of spatial gradients, that are not directly available if the PDF  $P_{u\psi}$  is known in a single point  $x$  only. Therefore, they have to be modeled. This is the

major difficulty associated with PDF Methods (Correa, 1995; Subramaniam and Pope, 1998). In the present work, a variant of the PDF method described by Eq. 14 is used. The PDF transport equation is integrated over the velocities space and the resulting PDF is the joint PDF of the scalars - species and enthalpy. Doing this, Eq. 14 becomes:

$$\begin{aligned} \bar{\rho} \frac{\partial}{\partial t} P_\phi(\psi; \mathbf{x}, \mathbf{t}) + \bar{\rho} \langle u_i \rangle \frac{\partial}{\partial x_i} P_\phi(\psi; \mathbf{x}, \mathbf{t}) + \frac{\partial}{\partial \mathbf{x}_j} \left[ P_\phi(\psi; \mathbf{x}, \mathbf{t}) \langle \mathbf{u}_j \rangle_{\phi=\psi} \right] \\ \sum_{\alpha=1}^{N_\alpha} \frac{\partial}{\partial \psi_\alpha} [\bar{\rho} P_\phi(\psi; \mathbf{x}, \mathbf{t}) \mathbf{S}_\alpha] = \sum_{\alpha=1}^{N_\alpha} \sum_{\beta=1}^{N_\beta} \frac{\partial^2}{\partial \psi_\alpha \partial \psi_\beta} \left[ \bar{\rho} P_\phi(\psi; \mathbf{x}, \mathbf{t}) \left\langle \mathbf{D} \frac{\partial \phi_\alpha}{\partial \mathbf{x}_i} \frac{\partial \phi_\beta}{\partial \mathbf{x}_i} \right\rangle \right]_\psi \end{aligned} \quad (15)$$

A conventional CFD code based on moment closure method is used to solve the mean equations for continuity, momentum and the turbulence model. In this work, a Second Order Closure model (Jones and Musonge, 1988) is used for turbulence. The solution of the PDF equation using conventional finite volume or finite difference methods would require a discretization over an 19-dimensional space: two dimensions in the physical space, two in the velocities space and fifteen in the space of scalar quantities (14 reactive species and enthalpy). Such a discretization is prohibitive owing to computational limitations. One can overcome this problem by means of stochastic methods. These methods model the evolution of the PDF by following the evolution of an ensemble of particles, which undergo a stochastic process. These particles are placed and fixed in the center of the grid cell. In this representation computational time increases linearly with the dimension of the scalar quantities space. Whereas in the finite-difference approach it would increase exponentially. The discretized scalar PDF transport equation at a cell P is given by

$$\begin{aligned} P_\psi^P(\psi, t + \Delta t) = & \underbrace{\left(1 - \frac{\Delta t}{\bar{\rho} \Delta Vol} A_P\right) P_\psi^P(\psi, t)}_{\text{I}} + \underbrace{\sum_{l=1}^{N_{nb}} \frac{\Delta t}{\bar{\rho} \Delta Vol} A_l P_\psi^l(\psi, t)}_{\text{II}} - \\ & \underbrace{\Delta t \sum_{\alpha=1}^{N_\alpha} \frac{\partial}{\partial \psi_\alpha} \left[ \rho P_\phi(\psi; \mathbf{x}, \mathbf{t}) \left\langle \frac{\partial \mathbf{J}_{i\alpha}}{\partial \mathbf{x}_i} \right\rangle \right]_{\mathbf{v}, \psi}}_{\text{III}} - \underbrace{\Delta t \sum_{\alpha=1}^{N_\alpha} \frac{\partial}{\partial \psi_\alpha} [\rho S_\alpha P_\phi(\psi; \mathbf{x}, \mathbf{t})]}_{\text{IV}} \end{aligned} \quad (16)$$

In the above equation, term I represents the instantaneous state of the PDF, term II models the influence of the convection and turbulent diffusion, term III gives the molecular diffusion and term IV the chemical reaction source term. Coefficients  $A_P$  and  $A_l$  in terms I and II come from the finite volume discretization of convection and diffusion terms. They are the same coefficients as in momentum equations. In the present work, the model IEM (*Interaction by Exchange with the Mean*) (Dopazo, 1975) is used for molecular transport (term III) of scalar quantities. It can be shown that in this model term III is equivalent to the evolution of the scalars quantities, which are modeled by:

$$\frac{\partial \phi_\alpha(t)}{\partial t} = -\frac{1}{2} C_\phi \langle \omega \rangle (\phi_\alpha(t) - \langle \phi_\alpha \rangle), \quad (17)$$

where  $\phi_\alpha$  is the scalars quantities vector,  $C_\phi$  is the constant of the IEM model,  $\langle \omega \rangle$  is the turbulence frequency,  $\phi_\alpha(t)$  is the value of the scalar quantity  $\alpha$  of the particle and  $\langle \phi_\alpha \rangle$  its mean value. Term IV represents the source term for each scalar (species and enthalpy). If the scalar is a reactive species  $\alpha$ , then  $S_\alpha$  stands for the chemical source term. The evolution equation, due the chemical reactions, can be given by:

$$\frac{\partial \phi_\alpha(t)}{\partial t} = S_\alpha(t), \quad (18)$$

where  $S_\alpha$  is the chemical source term for the species  $\alpha$ , evaluated from the thermochemical model. In the energy equation, the radiation source term acts on the entalpy  $h$  of the fluid. The entalpy evolution due the radiation source term is given by:

$$\frac{\partial h(t)}{\partial t} = \dot{q}(t), \quad (19)$$

where  $\dot{q}$  is given by the Eq .12.

One of the major advantages of the PDF method is that neither the chemical nor the radiation source terms have to be modeled as it is done in moment closure methods. However, even in PDF methods, it is a difficult task to incorporate a detailed chemistry model. The change in mass fraction of every species is calculated for

each stochastic particle by means of Eq. 18 above. For instance, a direct integration of Eq. 18, including a detailed mechanism with typically 15 species, would require approximately 18 months in a workstation. Previous simulations done in this work, with a mechanism containing 4 steps and 10 particles per cell, took 4 to 5 weeks for one test case, alone. Such CPU requirements render the development of detailed models for turbulent flames prohibitive. In the past, a number of reduction, storage and retrieval techniques have been employed to deal with the excessive computer time required. The most widely used approach in PDF methods is to use a reduced mechanism stored previously in a look-up table. (Hinz, 2000) has studied the flame presented in this work by using two variations of reduced mechanisms. The first one involved 4 global reactions and a second one with three parameters, based on the ILDM (*Intrinsic Low-Dimensional Manifolds*) strategies (Maas and Pope, 1992). Both reduced mechanisms were integrated and stored in a look-up table. During the simulation the change in concentrations for each species was recovered from the table. However, the use of a look-up table limits the chemistry model to three or four reactive species, which are insufficient to describe the combustion process adequately (Chen, 1997; Pope, 1997). As an alternative to both direct integration of Eq. 18 and look-up table, (Pope, 1997) has proposed the ISAT algorithm, whose essentials are described below.

### 6.1. ISAT ALGORITHM

The main idea in the ISAT algorithm is to integrate Eq. 18 only when it is necessary. That means only at the first time, when the stochastic event occurs. This is quite different from the look-up table approach, where a huge number of points in the table are, in fact, not used during the flame simulation. The essentials of the ISAT algorithm can be briefly exposed as follow.

- For the first particle representing the scalar PDF in a cell, Eq. 18 is integrated in time and both the initial state (defined by its mass fractions and enthalpy of the mixture) and the end state are stored in a binary tree. A region of high precision around the tabulated thermo-dynamic state is defined with a maximum departure of 5 % for each component. Within this region, linear approximation is assumed to be reasonable. It means that, for others queries lying within that region, no integration is performed and the answer - the end state - is obtained with a linear interpolation.
- For a new query , the binary tree is traversed and, if a node is found where the linear approximation is accurate, then this value is returned. Otherwise a new integration of Eq. 18 is performed and a new table entry is generated.
- The answer is assigned to the stochastic particle.

In this algorithm, a table is built up in situ, as the reactive flow calculation is performed. Only the accessed region of the composition space is stored. In the original algorithm proposed by Pope, 1997, there is a dynamic setting of the region of precision. In the present work, a simplified version is implemented. Here, a percent of departure from the tabulated state is heuristically fixed. An evaluation of the independence of the results from this parameter was performed. This simplified version avoids a large number of numerical matrix manipulations. The grid of the CFD/PDF code has (80x70 cells) with 100 stochastic particles per cell. The stochastic particles are assigned the properties of mass fraction of the reactive species and enthalpy. Mean profiles are evaluated after statistical convergence is achieved. To reduce stochastic fluctuations the mean properties were averaged over 100 iterations. Boundary conditions at inflow and outflow are defined according to physical boundary conditions of the jet flame. At the burner exit and pilot, the velocities and concentrations are taken from experimental data. At the coflow region only air is supplied. At the other boundaries a von Neumann condition was set for all variables.

## 7. Results

In this section, simulation results are presented and compared to experimental data. Velocity measurements were obtained from (Schneider and Geiss, 1999) and scalar data from (TNF, 1999a). In the following figures the the axial position ( $x$ ) is normalized by the tube diameter ( $D$ ). The velocity profile at the center line of the flame is shown in Fig. (1). Experimental data were obtained (Schneider and Geiss, 1999) with Laser Doppler Anemometry. The velocity field was computed with the well known fast chemistry approach (chemical equilibrium) and parameterized with the mixture fraction. The agreement with the experimental data is quite good. At the end of the flame the deviations become larger. With this velocity distribution the scalar joint PDF was computed.

In Fig. (2), the centerline evolution of the mixture fraction is plotted. The agreement between simulation and Raman-data (TNF, 1999a) is good. The mixture fraction is used only with the Presumed PDF/Fast Chemistry model (Janicka and Kollmann, 1979). The PDF/ISAT method does not use this quantity. It is computed from the species concentrations that were obtained by the PDF method. It is, however, a good indicator of the mixing process.

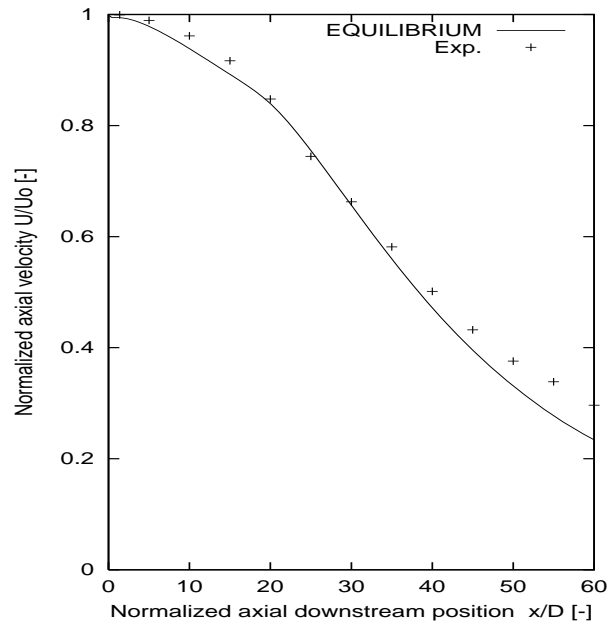


Figure 1: Centerline Axial velocity normalized with the nozzle exit velocity. Presumed PDF/Fast chemistry and LDA measurements (Schneider and Geiss, 1999)

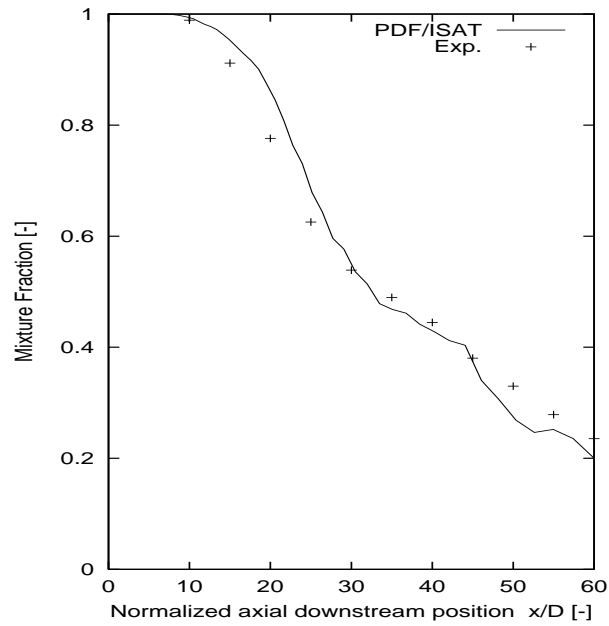


Figure 2: Favre averaged mixture fraction versus normalized flame axis  $x/D$ . Data from (TNF, 1999a) in comparison to prediction.

The axial temperature profile is presented in Fig. (3). There are shown both simulations: with and without radiation. The agreement with experimental mean values is good. The maximum temperature occurs at the position of the stoichiometric mixture fraction. This means that the flame length, if measured by the maximum temperature, is correctly predicted. As one can see, the model including radiation reduces the temperature by about 100K at maximum temperature. Although the temperature with the radiation model is closer to the experimental data, there is still a great departure between calculations and experiments before the peak of maximum temperature, .

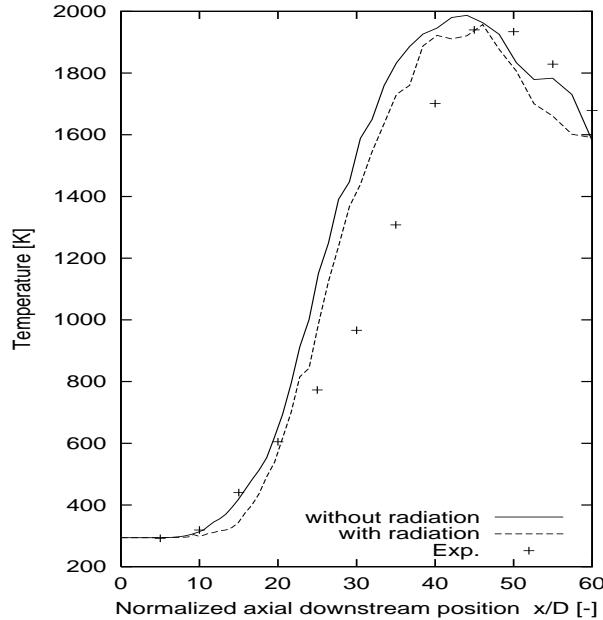


Figure 3: Favre averaged temperature versus normalized flame axis  $x/D$ . Data from (TNF, 1999a) in comparison to prediction.

The mean values of the species  $CO_2$  and  $CO$  at the axial downstream position are presented in the next two figures. The mass fraction of the major species  $CO_2$  (Fig. (4)) is an indicator of the whole combustion process. It is an important indicator of the energy conversion efficiency in the combustion system. The numerical results agree very well with the experimental data. This means that the flame structure, as far as major species are concerned, was captured. On the other hand, the mass fraction of  $CO$  (Fig. (5)) indicates the departure of complete combustion regime. The  $CO$  mass fraction is a measure of local extinction in the flame. Carbon monoxide is an intermediate species and, therefore, its prediction is very sensitive to the turbulent combustion model. Despite of the irregular mean profile, due probably to the low number of particles in the cells and to the approximation procedure in the ISAT algorithm, the  $CO$  formation is reasonably predicted by both models (with and without radiation). It can be said that the flame structure, concerning to local partial extinction, was captured. This is confirmed by the conditioned mean values of  $CO$  presented in the Fig. (8) and (9).

The radial mean values of temperature and carbon monoxide are presented in the Fig. (6) and Fig. (7) respectively. There are shown the profiles in two planes of the flame:  $x/D=30$  and  $x/D=60$ , for both models (with and without radiation). These planes were chosen because they represent two interesting flame regions: the near nozzle region, where the Damköhler number is low and the end of the flame, where the Damköhler number is high.

From the radial profile of temperature (Fig. (6)), one can see that the level of maxima temperature is achieved at both planes, but some deviations are observed. The width of the flame at the plane  $x/D=60$  is over-predicted by the simulation. This could be attributed to the second moment closure model used for the velocity-scalar correlation in the PDF Method (Eq.(15)). At the center line for the plane  $x/D=30$ , as already shown in Fig. (3), the temperature is over-predicted.

The radial profile for mass fraction of  $CO$  is shown in Fig. (7). Despite of the observed deviations, it can be said that the model is able to capture the main structure of the  $CO$  mean profile at the flame. At both plane, the calculated values are very close to the measured ones. The radial profile also agree well with the experimental data.

The conditioned mean values of  $CO$  and temperature are presented in the Fig. (8),(9) and (10). There are plotted all values of  $CO$  and temperature versus mixture fraction that have been detected in the radial planes. Presented are the conditioned mean values of  $CO$  and temperature at the radial planes  $x/D=30$  and  $x/D=60$ . The analysis with the conditioned mean value enables one to isolate the influence of convection and velocity-

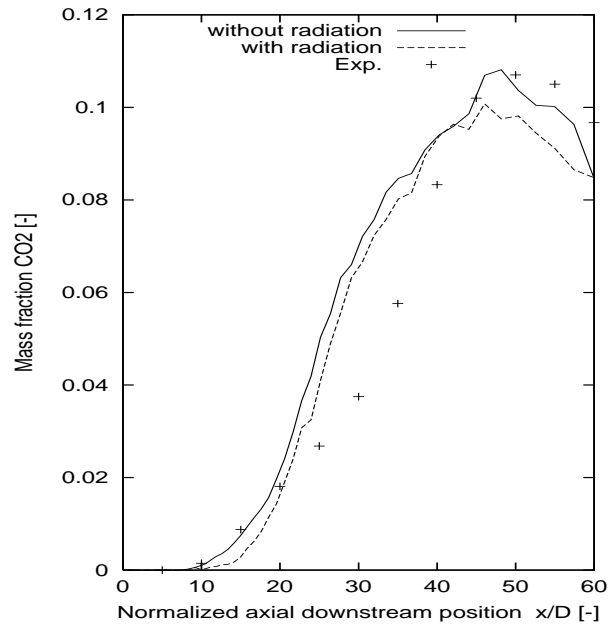


Figure 4: Favre averaged mass fraction of CO<sub>2</sub> versus normalized flame axis  $x/D$ . Data from (TNF, 1999a) in comparison to prediction.

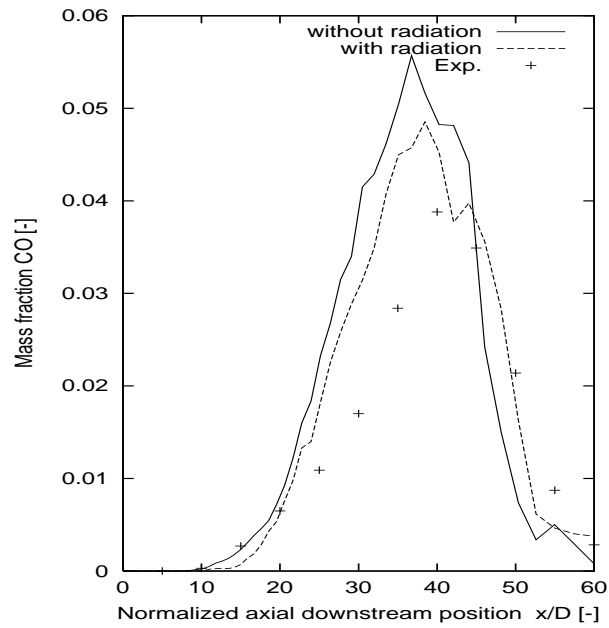


Figure 5: Favre averaged mass fraction of CO versus normalized flame axis  $x/D$ . Data from (TNF, 1999a) in comparison to prediction.



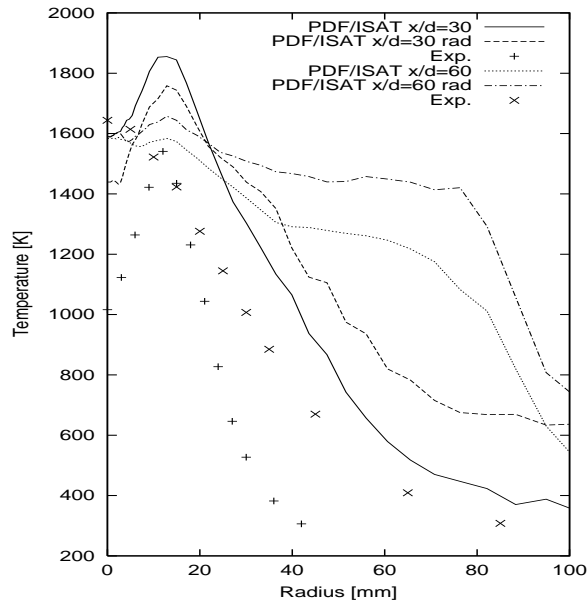


Figure 6: Favre averaged temperature versus radius. Data from (TNF, 1999a) in comparison to prediction.

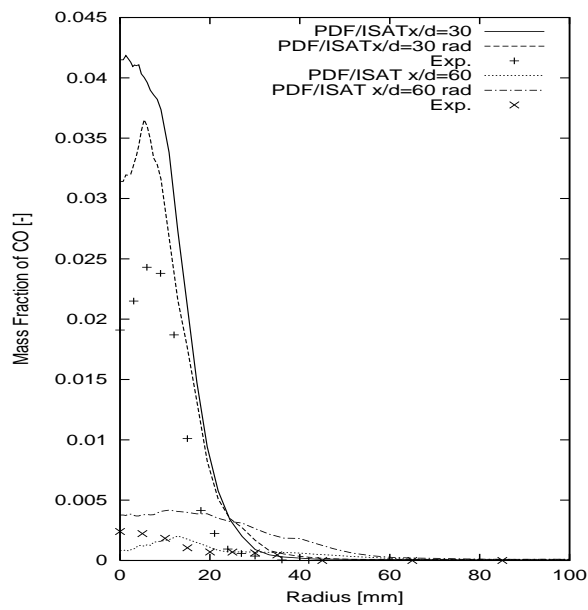


Figure 7: Favre averaged CO mass fraction versus radius. Data from (TNF, 1999a) in comparison to prediction.

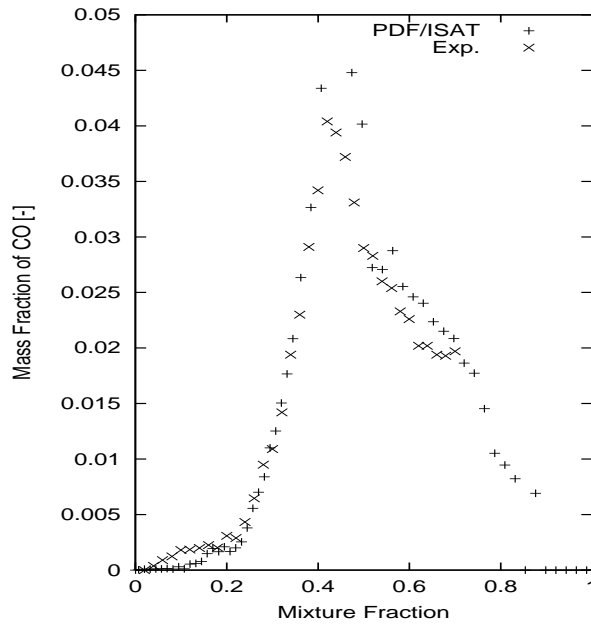


Figure 8: Favre conditioned mean value of CO at the plane  $x/D=30$ . Data from (TNF, 1999a) in comparison to prediction.

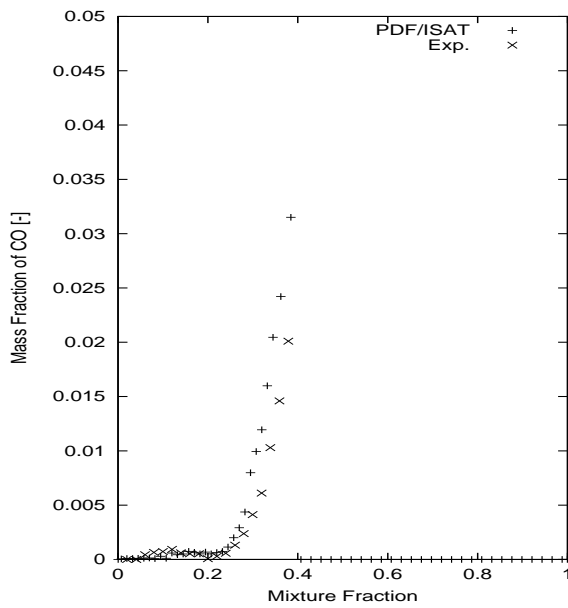


Figure 9: Favre conditioned mean value of CO at the plane  $x/D=60$ . Data from (TNF, 1999a) in comparison to prediction.

scalar correlation on the mean values. In the axial and radial profiles of concentration and temperature shown in the preceding figures, it is not possible to identify individually what physical process causes the deviations from the measured values. In the conditioned mean values, one can evaluate the effect of both chemical reactions and molecular mixing model on the mean values of CO and temperature. The main information that can be extract from these figures is how near to the complete combustion a stochastic particle, which has a certain mixture fraction, has reacted. If the conditioned mean value of carbon monoxide CO, for a given mixture fraction, is lower than the measured value, it means that the detailed chemistry mechanisms together with the molecular mixing model have under-predicted the extinction phenomena. More difficult is to evaluate where the under-prediction comes from, whether from the chemistry mechanisms or from the mixing model. In the implemented algorithm, mixing model and chemistry reactions are carried out as subsequent numerical procedures. The correct coupling of both steps is a very known drawback (Dopazo, 1975; Correa, 1995) with the PDF Method.

The mean values of CO conditioned by the mixture fraction, at the planes  $x/D=30$  and  $x/D=60$ , are presented at the Fig. (8) and (9) respectively. The numerical results agree very well with the measured conditioned values. At both planes, in other words at different Damköhler Number, the turbulent combustion model was able to capture the flame structure.

The conditioned mean values of temperature at the planes  $x/D=30$  and  $x/D=60$  are shown in Fig. (10). It can be seen that the agreement between numerical and experimental data is good. At the plane  $x/D=30$ , on the rich side of the flame, one can observe that the numerical method systematically over-predict the temperature. This is, at least, consistent with the higher values shown in Fig. (3) and Fig. (6). At the plane  $x/D=60$ , however, the agreement is very good.

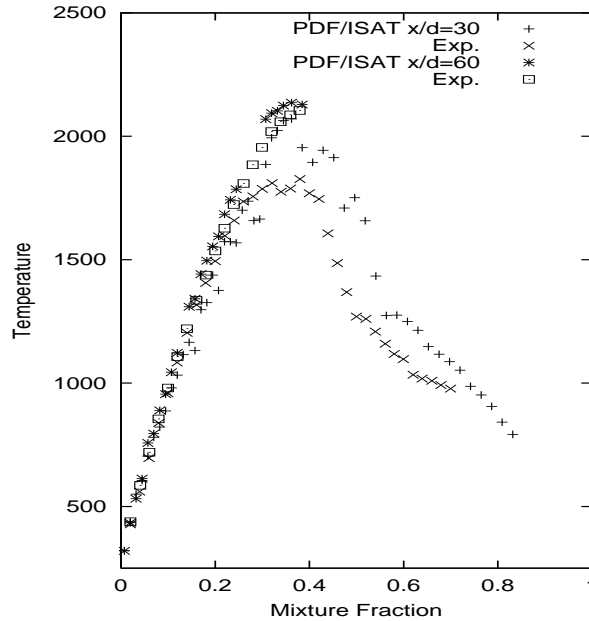


Figure 10: Favre conditioned mean value temperature for planes  $x/D=30$  and  $x/D=60$ . Data from (TNF, 1999a) in comparison to prediction.

The instantaneous values of temperature versus the mixture fraction at the two radial planes are presented in Fig. (11) and Fig. (12). It can be seen that extinction effects occur at the plane  $x/D=30$  (Fig. (10)), but not at plane  $x/D=60$  (Fig. (12)). It is however not clear, why the conditioned mean values of temperature at the plane  $x/D=30$  (Fig. (10)) is over-predicted. One could suspect that the model is not able to capture extinction. This is, however, not consistent neither with the CO mass fraction (Fig. (8)) nor with the temperature itself (Fig. (11)), where clearly extinction is observed. Previous work (Krieger, 2002) suspects that heat losses due radiation from the flame could also reduce the temperature. It is however not clear, why should radiation play an important role at the base of the flame ( $x/D=30$ ), but not at the end ( $x/D=60$ ). This effect was accounted for in this work and no significant improvement of the temperature predictions were observed.

## 8. Conclusions

The main goal of the present work was to investigate the structure of a turbulent methane flame. In order to do this, a PDF Method with the ISAT algorithm was implemented. This made it possible, to use a detailed chemistry mechanism with 14 species and radiation heat losses. The main conclusions of this work are: The PDF allows one to perform a simulation without the need of modelling the average source term, as it is necessary

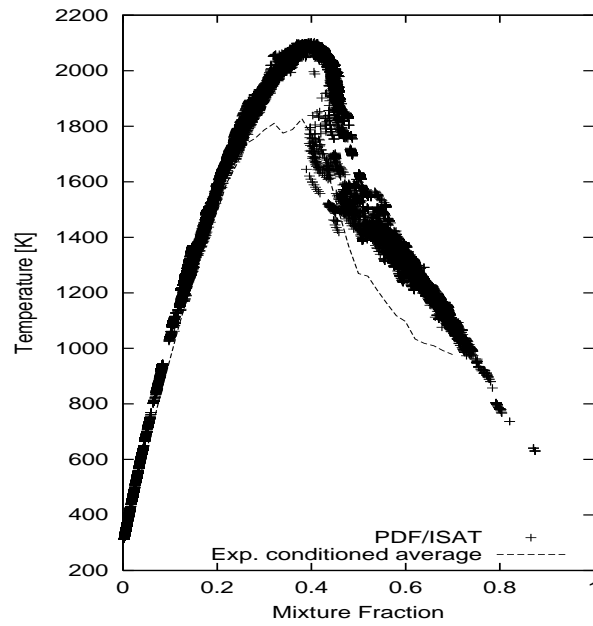


Figure 11: Scatter plot of temperature versus mixture fraction at planes  $x/D=30$

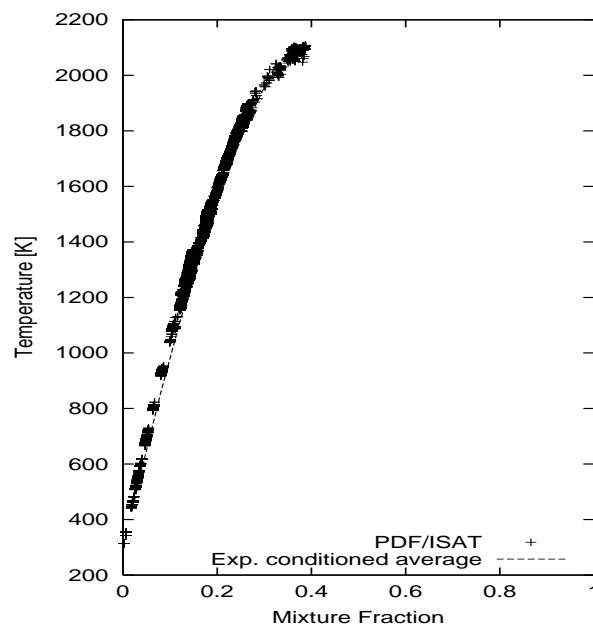


Figure 12: Scatter plot of temperature versus mixture fraction at planes  $x/D=60$ .

in the Presumed PDF and statistical moments models. Global aspects of the flame structure like maximum levels of temperature, flame length, concentration of major species and carbon monoxide were captured with acceptable agreement to experimental data. The extinction effects were captured, as seen in the conditioned mean values of carbon monoxide and temperature. Some deviations on mean values and conditioned mean values were however observed, although radiation effects were taken into account. Possible causes to this deviations are: the model of turbulent transport in both the second order model to the Reynolds stress tensor and in the PDF transport equation and/or a more complex thermochemical model should be used.

## 9. Acknowledgements

The author would like to thank FAPESP - São Paulo, Brazil for sponsoring this project and TU-Darmstadt and Sandia National Laboratories for providing the experimental data sets.

## 10. References

- Barlow, R. S. e. a., 2001, Scalar Profiles and NO Formation in Laminar Opposed-Flow Partially Premixed Methane/Air Flames, "Combustion and Flame", Vol. 127, pp. 2102–2118.
- Chen, J.-Y., 1997, Development of Reduced Mechanisms for Numerical Modelling of Turbulent Combustion, Workshop on Numerical Aspects of Reduction in Chemical Kinetics.
- Correa, S. M., 1995, A Direct Comparison of Pair-Exchange and IEM Models in Premixed Combustion, "Combustion and Flame", Vol. 103, No. 3, pp. 194–206.
- Dopazo, C., 1975, Probability Density Function Approach for a Turbulent Axisymmetric Heated Jet. Centerline Evolution, "Physics of Fluids", Vol. 4, No. 18, pp. 397–404.
- Hinz, A., 2000, "Numerische Simulation turbulenter Methan-diffusionsflammen mittels Monte Carlos PDF Methoden", PhD thesis, TU-Darmstadt, Germany.
- Janicka, J. and Kollmann, W., 1979, A Two-Variables Formalism for the Treatment of Chemical Reactions in Turbulent H<sub>2</sub>-Air Diffusion Flames, "Proceedings of the 17th. Symposium (Intl) on Combustion", pp. 421–430, Pittsburgh, USA.
- Jones, W. P. and Musonge, P., 1988, Closure of the Reynolds stress and scalar flux equations, "Physics of Fluids", Vol. 31, No. 12, pp. 3589–3604.
- Krieger, G., 2002, Numerical Simulation of Local Extinction in a Turbulent Non-Premixed Methane Flame, "Proceedings of the ENCIT 2002", Vol. CD-ROM, Caxambu-MG.
- Kuo, K. K., 1986, "Principles of Combustion", John Wiley & sons.
- Maas, U. and Pope, S. B., 1992, Simplifying Chemical Kinetics: Intrinsic Low-Dimensional Manifolds in Composition Space, "Combustion and Flame", Vol. 88, pp. 239–264.
- Magnussen, B. F. and Hjertager, H., 1976, On Mathematical Modeling of Turbulent Combustion with Special Emphasis on Soot Formation and Combustion, "Proceedings of the 16th. Symposium (Intl) on Combustion", Vol. 1, pp. 719–729, Pittsburgh, USA.
- Pope, S. B., 1985, PDF Methods for Turbulent Reactive Flows, "Progress in Energy and Combustion Science", Vol. 11, pp. 119–192.
- Pope, S. B., 1997, Computationally Efficient Implementation of Combustion Chemistry using In Situ Adaptive Tabulation, "Combustion Theory Modelling", Vol. 1, pp. 41–63.
- Schneider, C. and Geiss, S., 1999, <http://www.ca.sandia.gov/tdf/Workshop>.
- Subramaniam, S. and Pope, S. B., 1998, A Mixing Model for Turbulent Reactive Flows based on Euclidean Minimum Spanning Trees, "Combustion and Flame", Vol. 115, pp. 487–514.
- TNF, 1999a, 4th. International Workshop on Measurement and Computation of Turbulent Nonpremixed Flame, <http://www.ca.sandia.gov/tdf/4thWorkshop/TNF4.html>.
- TNF, 1999b, International Workshop on Measurement and Computation of Turbulent Nonpremixed Flame, <http://www.ca.sandia.gov/tdf/Workshop>.
- Turns, S. R. and Myhr, F. H., 1975, Oxides of Nitrogen Emissions from Turbulent Jet Flames: Part I - Fuel Effects and Flame Radiation, "Combustion and Flame", Vol. 4, No. 3-4, pp. 319–335.